10th ANKARA INTERNATIONAL AEROSPACE CONFERENCE **AIAC-2019-066**
18-20 September 2019 - METU, Ankara TURKEY

LONGITUDINAL AUTOMATIC LANDING CONTROLLER DESIGN BY USING OPTIMIZATION METHODS

Emre Can Suicmez* and Ali Turker Kutay†
METU
Ankara, Turkey

ABSTRACT

Longitudinal automatic landing controller for a transport aircraft is designed by combining classical loop closure approach with optimization methods. With the help of optimization methods, controller is designed to satisfy predefined time and frequency domain requirements without extensive tuning effort. Actuator dynamics are included into the design by defining augmented state space forms. Design of the controller and simulations are performed in MATLAB/Simulink environment. Controller is tested by adding sensor delays that is expected to be handled based on frequency domain requirements. Results show that time and frequency domain requirements are satisfied in nonlinear simulations.

DEFINITIONS & ABBREVIATIONS

θ : Pitch angle
α : Angle of attack
q : Roll rate
V : Airspeed
γ : Flight path angle(FPA)
γ_R : Reference glide path angle
h : Altitude
V_A : Aircraft velocity tangential to glide slope
V_{cmd} : Airspeed command
θ_{cmd} : Pitch angle command
h_{cmd} : Altitude command
δ_T : Throttle actuator input
$\delta_{T,act}$: Throttle actuator output
δ_e : Elevator actuator input
$\delta_{e,act}$: Elevator actuator output
SAS : Stability Augmentation System
$DGPS$: Differential Global Positioning Systems

*PhD Student in Aerospace Engineering, Email: e156123@metu.edu.tr
†Asst. Prof. Dr. in Aerospace Engineering, Email: kutay@metu.edu.tr

INTRODUCTION

Automatic landing systems has been used in aircraft industry since 1965s [Juang J.G. and Chio J.Z. , 2005]. It is a very crucial part of flight since achieving a safe landing without disturbing passengers in severe weather conditions(wind, gust et.) is a challenging problem. In literature there are many works about auto-landing problem and it is stated that most of the conventional controllers are based on gain scheduling [Buschek H. and Calise A.J. , 1997]. There are more recent studies that use modern control approaches such as fault-tolerant[Liao F., Wang J.L. et al. , 2005], adaptive, fuzzy logic[Juang J.G. and Chio J.Z. , 2005] or nonlinear energy minimization based controllers [Akmeliawati R. and Mareels I.M.Y. , 2010].

In this study, longitudinal auto-landing problem is solved by combining classical cascaded loop closure approach with optimization methods applied in MATLAB. Controller is designed by considering actuator dynamics. Parameters of each control loop is obtained by optimization techniques to satisfy predefined design requirements which greatly reduce tuning effort. Design requirements include transient characteristics and also stability margins such as gain,phase or delay margin. To check stability margins, controller is tested by adding sensor delay in pitch angle measurement.

Automatic landing control problem for longitudinal motion is divided into two phases: glide-path control and flare control. First, the inner loop pitch attitude hold controller is designed, then outer loop speed hold and altitude tracker autopilots are designed. Desired trajectory is generated by using a altitude command generator by considering smooth transition between glide-path and flare trajectories.

GLIDE PATH & FLARE CONTROLLER

Tracking desired glide-path trajectory requires simultaneous control of thrust and pitch attitude [Blakelock J.H. , 1991], [Stevens B.L., Lewis F.L. and Johnson E.N. , 2016]. It is highly possible to stall the A/C by only using elevator control to track desired glide-path trajectory [Stevens B.L., Lewis F.L. and Johnson E.N. , 2016]. Therefore, both engine thrust and elevator inputs have to be adjusted carefully to achieve a safe landing.

Glide-slope geometry of a typical landing system can be seen in Figure 1. By using a radio beam placed at point Q and an equipment on aircraft, perpendicular distance d of aircraft from the desired glide-path can be measured [Stevens B.L., Lewis F.L. and Johnson E.N. , 2016]. Highly accurate DGPS systems are also used directly or to assist auto-landing [Brown R., Romrell G. et al. , 1996].

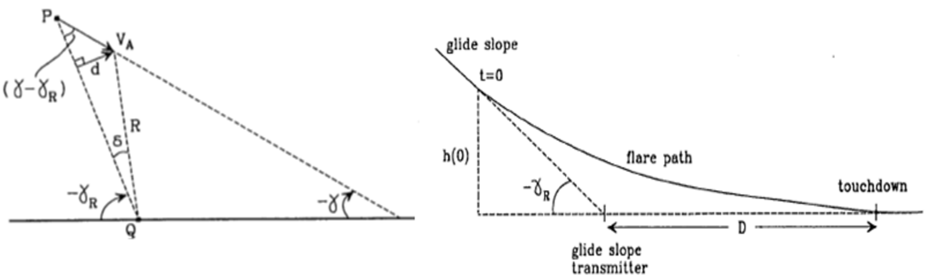

Figure 1: Glide slope and flare trajectories for typical autolanding. Figure taken in the courtesy of [Stevens B.L., Lewis F.L. and Johnson E.N. , 2016].

Using the geometric and dynamic relations, the perpendicular distance d and its derivative $\dot{d}$ are obtained as follows [Stevens B.L., Lewis F.L. and Johnson E.N. , 2016]:

$$\left.\begin{aligned} d &= Rsin(\delta) \\ \dot{d} &= V_A(\gamma - \gamma_R) \end{aligned}\right\} \tag{1}$$

Longitudinal controller tries to track desired trajectory by adjusting elevator and throttle control inputs. It should be noted that aircraft velocity that is tangential to glide-slope V_A exists in $\dot{d}$ equation and $\dot{d}$ can be inserted into linearized state-space equations as a state.

The framework of the longitudinal autolanding controller is given in Figure 2. As can be seen, throttle and elevator channels are decoupled and throttle tries to hold desired airspeed at value above stall velocity while elevator is used to track desired landing trajectory(glide-path + flare). Alternatively, elevator input can be used to hold a predefined flight path angle.

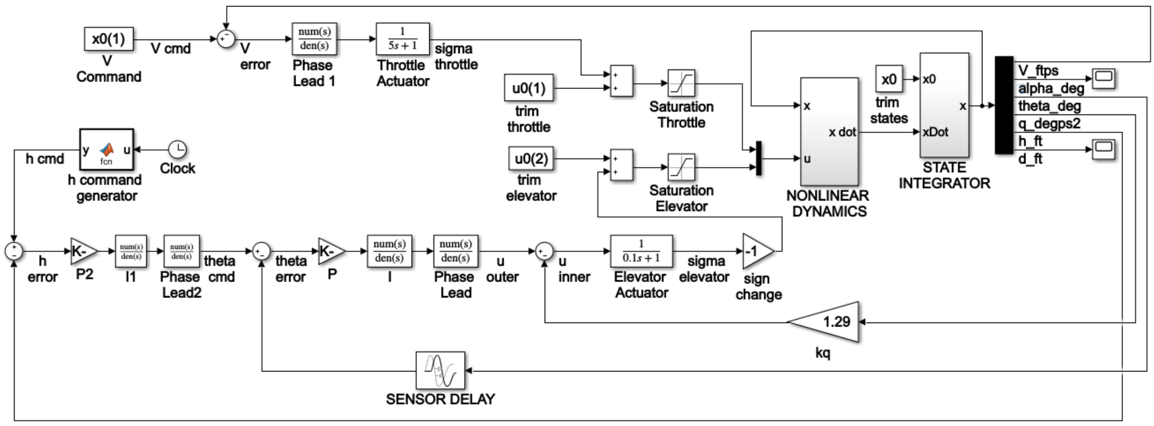

Figure 2: Simulink model of longitudinal autolanding controller.

Elevator and throttle servos are modeled as first order-lag systems with 0.1 and 5 seconds lag time as following [Stevens B.L., Lewis F.L. and Johnson E.N. , 2016]:

$$G_{\delta_T} = \frac{\delta_{T,act}}{\delta_T} = \frac{1}{5s+1} \ , \ G_{\delta_e} = \frac{\delta_{e,act}}{\delta_e} = \frac{1}{0.1s+1} \tag{2}$$

The nonlinear dynamic model of a transport aircraft in landing configuration is given in page 180 of [Stevens B.L., Lewis F.L. and Johnson E.N. , 2016]. This model is used in simulations to verify the controller and to obtain linearized state space forms for controller design.

Before designing outer loop compensators, first an inner loop pitch attitude hold autopilot will be designed.

Pitch Attitude Hold Autopilot

Pitch hold autopilot is first designed as an inner loop for automatic landing controller(Figure 2).

By using the nonlinear model for transport aircraft given in [Stevens B.L., Lewis F.L. and Johnson E.N. , 2016], A/C is trimmed at landing configuration such that landing gear and flaps are deployed at $V = 250\ ft/s$, $h = 50\ ft$ and $\gamma = -2.5\ deg$. Pitch attitude hold autopilot is expected to give fast enough inner loop response at flare maneuver, so that it is designed by using the model linearized at the beginning of flare ($h = 50\ ft$).

As mentioned previously, to account into the servo delay, the elevator actuator is modelled as a first order system with 0.1 seconds time constant (% 95 of the input is reached at 0.3 seconds). To include actuator effects into controller design, a new state space model is obtained by adding actuator states into state space representation as following:

$$\left.\begin{array}{c} \dot{x} = Ax + Bu, \ \ y = Cx, \ \ with \ \ x = [\delta_{e,act}, \ V, \ \alpha, \ \theta, \ q]^T \ \ u = \delta_e \\ A = \begin{bmatrix} -10 & 0 & 0 & 0 & 0 \\ 0 & -0.0389 & 18.99 & -32.14 & 0 \\ 0 & -0.001 & -0.645 & 0.0056 & 1 \\ 0 & 0 & 0 & 0 & 1 \\ 0.1099 & 0 & -0.773 & -0.0008 & -0.529 \end{bmatrix} \ B = \begin{bmatrix} 1 \\ 0 \\ 0 \\ 0 \\ 0 \end{bmatrix} \ C = \begin{bmatrix} 0 & 0 & 0 & 57.3 & 0 \\ 0 & 0 & 0 & 0 & 57.3 \end{bmatrix} \end{array}\right\} \tag{3}$$

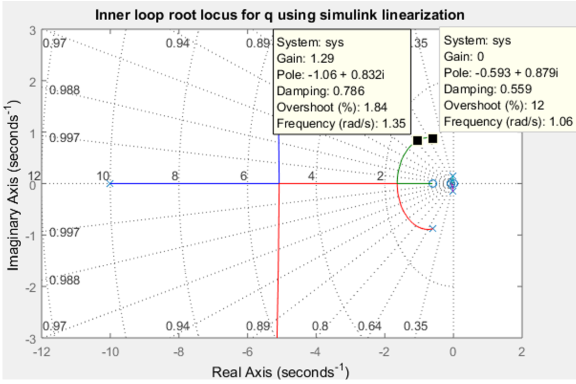

Figure 3: Root locus plot for inner loop q feedback.

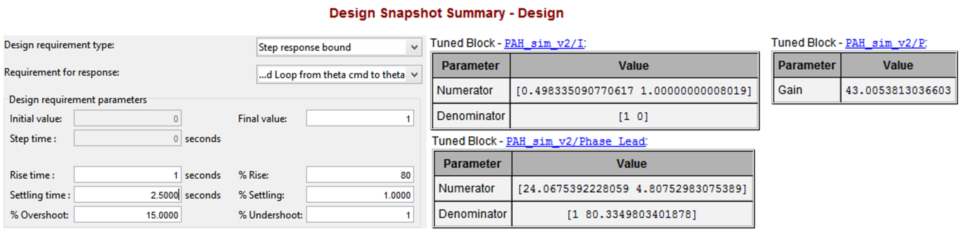

Figure 4: Pitch hold autopilot outer loop design constraints and results of optimization for P,I and Phase Lead compensator.

The overall scheme of pitch attitude hold controller is given in Figure 2. First, inner pitch rate (q) loop is closed and then PI+Phase Lead Compensator is tuned to obtain satisfactory θ response. Inner pitch rate loop acts like the derivative action and increases the damping of the short period mode for faster response. As mentioned previously, inner pitch rate loop can be considered as SAS, therefore it is the first design step. Then PI + Phase lead compensator is designed to obtain satisfactory θ response. Root locus method is used to tune inner pitch rate loop feedback(k_q) and Control System Design Tool of MATLAB is used to tune PI+ Phase lead compensator. Time domain design constraints are defined and optimization is used to obtain final controller parameters that satisfy design constraints.

By using linearized dynamics given in Equation set (3), open loop damping values for short period and phugoid mode are found as 0.559 and 0.0875, respectively. To increase short period damping by adding q feedback loop, root locus plot of $\frac{q}{\delta_e}$ is used (Figure 3). Our aim is achieving damping ratio greater than 0.78 and so feedback gain of 1.29 satisfy this requirement according to Figure 3. This value is good enough to achieve fast response in flare maneuvers [Stevens B.L., Lewis F.L. and Johnson E.N. , 2016].

Once inner pitch rate controller is closed, outer loop can be designed by tuning the proportional(P), Integral(I) and Phase Lead controllers (Figure 2). "Control System Designer" tool of MATLAB/Simulink is used to tune parameters via optimization. Performance constraints/requirements are defined at first and optimization is used to obtain controller parameters.

Step response from θ_{cmd} to θ is constraint to have 1 seconds rise time, 2.5 seconds settling time (with % 1 criteria) and % 15 maximum overshoot . In addition steady state value is constraint to be 1. All of these constraints are defined in "Design Requirements" tab of Control System Designer tool (Figure 4). Optimization is performed by using "Gradient descent" method with "Active-Set" algorithm.

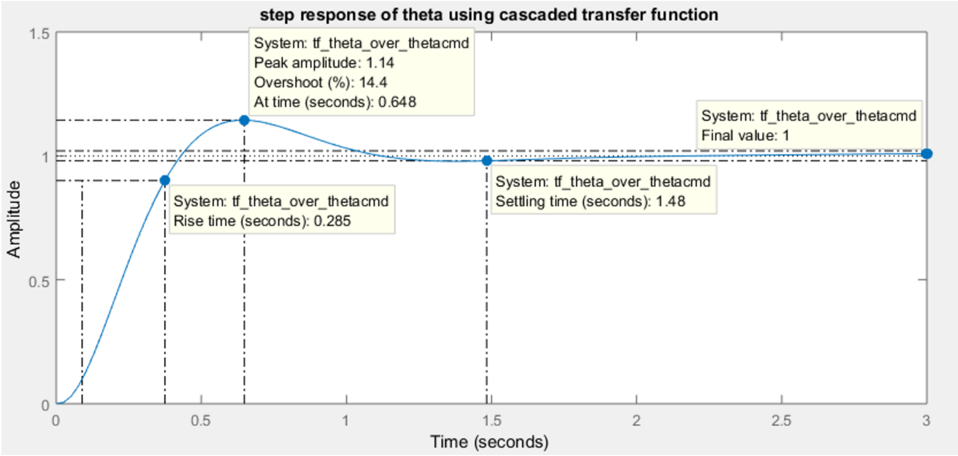

Figure 5: Transient characteristics of pitch hold autopilot.

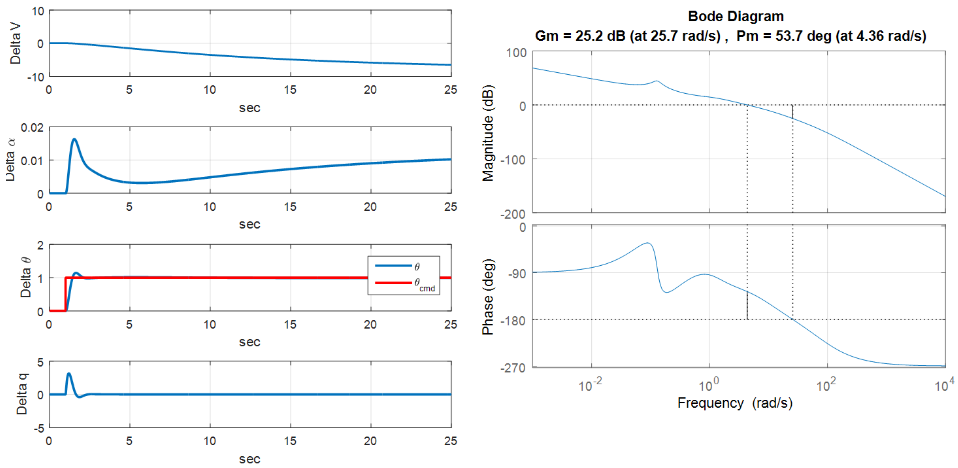

Figure 6: Pitch hold autopilot stability margin and step response.

To examine transient characteristics of overall pitch hold autopilot, step input response of $\dfrac{\theta}{\theta_{cmd}}$ transfer function that is given in Figure 5. According to Figure, rise time is 0.285 sec., maximum overshoot is % 14.4, settling time is 1.48 sec. and steady state value of θ is equal to 1. These values are within the limits that are predefined in constraint optimization process Figure 4. In other words, transient performance of pitch hold autopilot is satisfactory.

Responses of all outputs $[V,\ \alpha,\ ,\theta,\ q]$ to unit step θ_{cmd} are also plotted in Figure 6. It can be seen that θ tracks unit step θ_{cmd} but there exist deviation in V since speed hold autopilot is not designed yet. It is noted that linearized model taken from [Stevens B.L., Lewis F.L. and Johnson E.N. , 2016] represents the deviation from trim condition.

Stability margins are also analyzed to check robustness. MATLAB's "margin" command is used and Phase & Gain margins for θ loop are given in Figure 6. Phase and gain margins are high enough to satisfy robustness requirements.

In conclusion, overall pitch attitude hold autopilot designed in this section has satisfactory transient response characteristics and stability margins are also high/safe enough (Figure 6). Next step is designing Speed Hold Autopilot to avoid stall during landing.

Speed Hold Autopilot

It is noted that, the linearized state space model used in pitch attitude hold autopilot was trimmed at $h = 50ft$ by considering fast maneuvers that might occur in flare. However, speed hold autopilot is expected to work in glide-path tracking, therefore linearized state space model that will be used in speed hold autopilot is trimmed at $h = 750ft$(beginning of the glide-path tracking), $V = 250ft$ and $\gamma = -2.5deg$. Following equation set represents the state space form of A/C dynamics without actuator dynamics:

$$\left.\begin{aligned} &\dot{x} = Ax + Bu, \quad y = Cx, \quad with \ x = [\ V,\ \alpha,\ \theta,\ q,\ h,\ d]^T \quad u = [\delta_e, \delta_T] \\ &A = \begin{bmatrix} -0.0386 & 18.984 & -32.139 & 0 & 0.0001 & 0 \\ -0.001 & -0.6325 & 0.0056 & 1 & 0 & 0 \\ 0 & 0 & 0 & 1 & 0 & 0 \\ 0.0001 & -0.759 & -0.0008 & -0.518 & 0 & 0 \\ -0.0436 & -249.8 & 249.8 & 0 & 0 & 0 \\ 0 & -250 & 250 & 0 & 0 & 0 \end{bmatrix} \quad B = \begin{bmatrix} 10.1 & 0 \\ -0.0002 & 0 \\ 0 & 0 \\ 0.0247 & -0.0108 \\ 0 & 0 \\ 0 & 0 \end{bmatrix} \quad C = \begin{bmatrix} 1 & 0 & 0 & 0 & 0 & 0 \\ 0 & 57.3 & 0 & 0 & 0 & 0 \\ 0 & 0 & 57.3 & 0 & 0 & 0 \\ 0 & 0 & 0 & 57.3 & 0 & 0 \\ 0 & 0 & 0 & 0 & 1 & 0 \\ 0 & 0 & 0 & 0 & 0 & 1 \end{bmatrix} \end{aligned}\right\} \quad (4)$$

Since pitch attitude autopilot is designed at first, the effect of this autopilot should be included into linear model that will be used in the design of speed hold autopilot. By this way coupling between pitch attitude and speed autopilots will be considered. Then, to obtain linearized state space model with throttle actuator and pitch attitude autopilot included, Simulink Linear Analysis Tool is used [Mathworks , 2017]. Following Simulink model is used to obtain state space model with embedded actuator models and inner loop pitch hold autopilot.

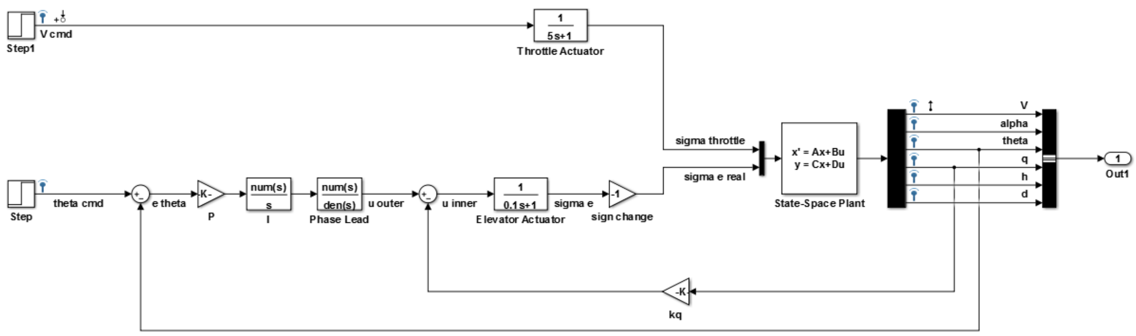

Figure 7: Simulink model to obtain linearized state space form that is used in speed hold autopilot design.

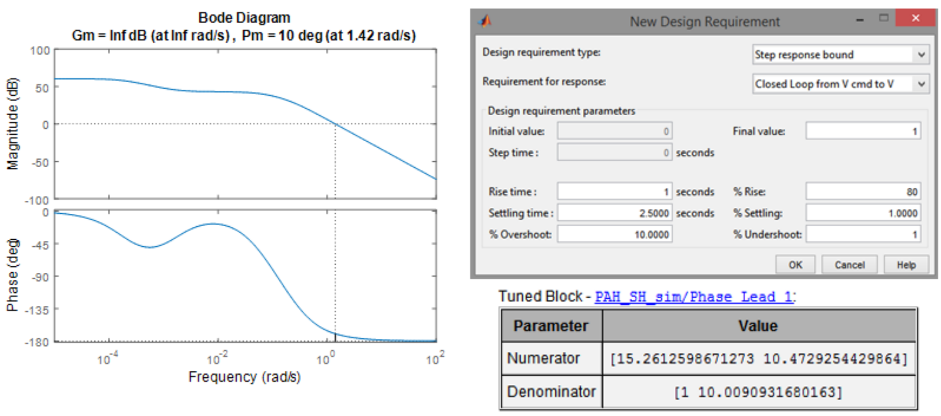

Figure 8: Bode plot of open loop transfer function V/V_{cmd}, design requirements and optimization results of phase lead compensator for speed hold autopilot.

As can be seen in Figure 7, V_{cmd} is selected as open loop input point and V is selected as open loop output. By looking at margins of open loop transfer function of V/V_{cmd}, it is seen that gain margin is infinity and phase margin is 10 degrees(Figure 8). For this reason a phase lead compensator is designed to increase phase margin. Similar approach used in pitch hold autopilot is used and optimization is performed to satisfy transient performance requirements defined in Figure 8 and also phase margin greater than 60 degrees.

To verify the designed controller step response of the closed loop transfer function V/V_{cmd} and bode plot of the open loop transfer function V/V_{error} is plotted in Figure 9. It is seen that desired transient characteristics are satisfied while phase margin is increased above 60 degrees.

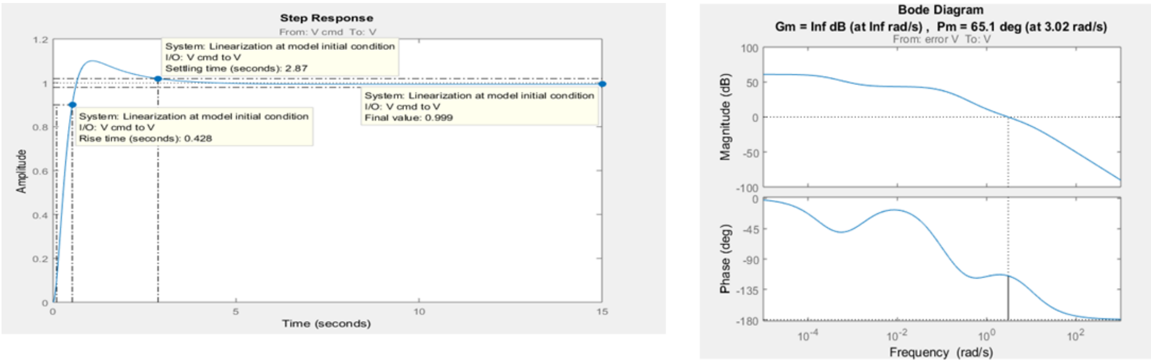

Figure 9: Transient characteristics and margins of speed hold autopilot.

To conclude, speed hold autopilot is designed by using a phase lead compensator since the main problem was the low phase margin of the speed channel. Next step is designing the outer loop altitude hold autopilot which is the last step of the longitudinal automatic landing controller.

Altitude Hold Outer Loop Autopilot

The final loop that will be closed is the altitude hold autopilot. Simulink model is linearized to obtain h/h_{cmd} open loop transfer function that includes both pitch attitude and speed hold autopilots, and also actuator dynamics. It is seen that $h/hcmd$ transfer function has stable poles; however, according to the bode plot stability margins are very low (Figure 10).

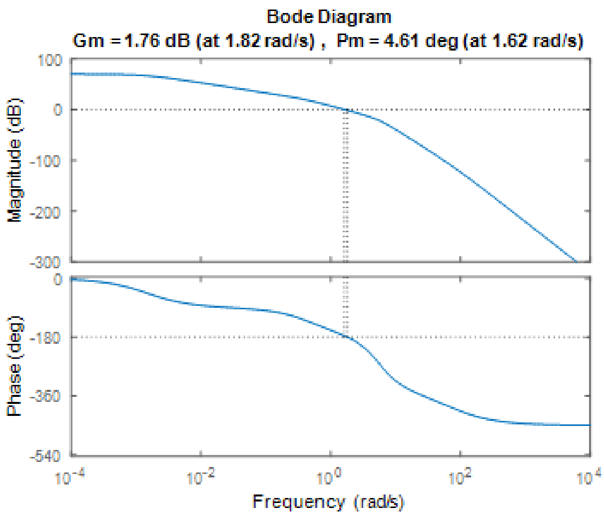

Design Snapshot Summary - Design

Tuned Block - PAH_SH_AltH_sim/I1:

Parameter	Value
Numerator	[0.154185472844267 0.0999999999854036]
Denominator	[1 0]

Tuned Block - PAH_SH_AltH_sim/P2:

Parameter	Value
Gain	0.990616476865746

Tuned Block - PAH_SH_AltH_sim/Phase_Lead2:

Parameter	Value
Numerator	[22.7305429390938 -0.13945487229828]
Denominator	[1 7.0217417733381]

Figure 10: Bode plot of open loop transfer function h/h_{cmd} and optimization results of PI + Phase lead compensator for altitude hold autopilot.

Then a Proportional Integral(PI) + Phase Lead compensator controller is designed for altitude hold purposes. Similar optimization based tuning techniques used in previous subsections are used to obtain controller parameters (Figure 10).

By using open loop transfer function h/h_{error}, stability margins of altitude loop is obtained as in Figure 11. It can be seen that gain margin is increased to 9.99 dB from 1.76 dB and phase

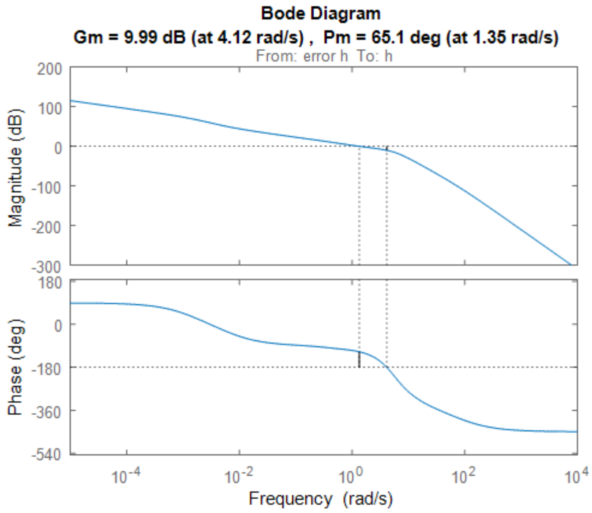

Figure 11: Margins of altitude hold autopilot.

margin is increased to 65.1 deg from 4.61 deg. Gain margin(9.99 dB) is above 6 dB and phase margin(65.1 deg) is above 45 dB which are safe/high enough for our system.

Once the altitude hold autopilot is designed, longitudinal autolanding controller design is completed. Next section gives simulation results of overall controller.

SIMULATION RESULTS

To test the controller, a glide-path and flare trajectory is generated at first. Glide-path trajectory is a straight line and the flare is trajectory is exponential to obtain a soft landing. Simulations are performed by using the nonlinear dynamics of transport aircraft given in page 180 of [Stevens B.L., Lewis F.L. and Johnson E.N. , 2016]. Throttle is limited between 0.15 and 1, which corresponds to motor idle and full throttle. Elevator actuator is limited between -15 and + 15 degrees.

According to Figure 6, pitch hold autopilot has 53.7 degree phase margin at 4.36 rad/s which corresponds to 0.21 sec delay margin. So, it is expected that autopilot should handle delay on pitch angle measurements at some level. To test delay margin, 0.1 seconds transport delay is added to nonlinear simulations (Figure 2).

First, autopilot is tested with no delay on pitch angle measurements(Figure 12) and then 0.1 seconds delay is added to pitch angle measurements (Figure 13). According to Figures 12 and 13, desired glide-path and flare trajectory is tracked accurately and aircraft lands smoothly. In landing, the challenging part is tracking the exponential trajectory at flare maneuver. It is seen that controller performance is satisfactory at flare which starts at 120 seconds(50 ft).

According to Figure 13, 0.1 second delay on pitch angle measurement is handled well. Delay cause elevator actuator to be more aggressive;however, it does not cause unstability at pitch channel. It is noted that 0.1 second delay is large enough by considering todays sensor technology. To conclude, increased phase margin in autopilot design makes system robust against sensor delays.

CONCLUSION

In this paper, longitudinal autolanding controller is designed for a transport aircraft by using optimization techniques in classical cascaded loop autopilot structure. Each loop is designed to achieve desired time and frequency domain requirements. Actuator dynamics are embedded into controller design to handle limiting effects of actuator dynamics. Controller is designed to

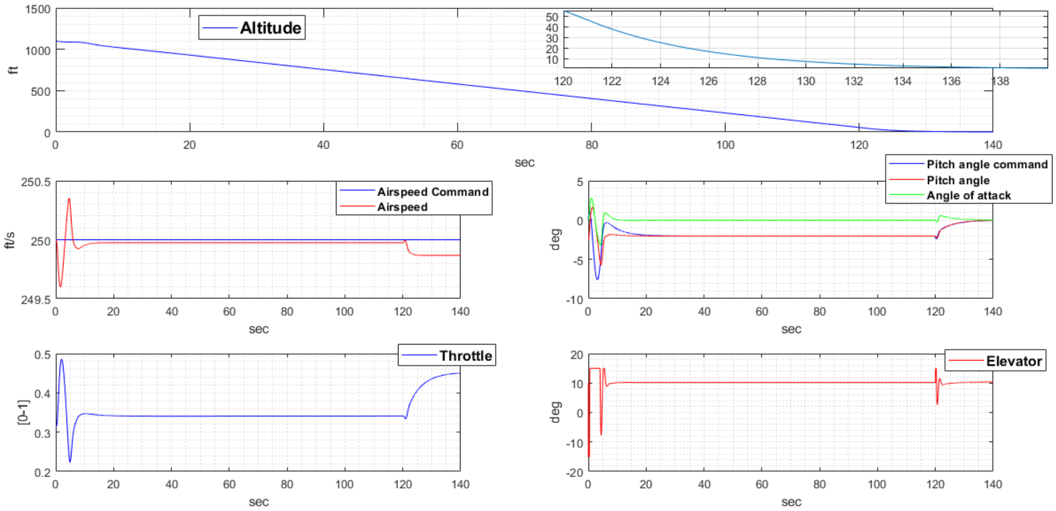

Figure 12: Simulation results for zero delay.

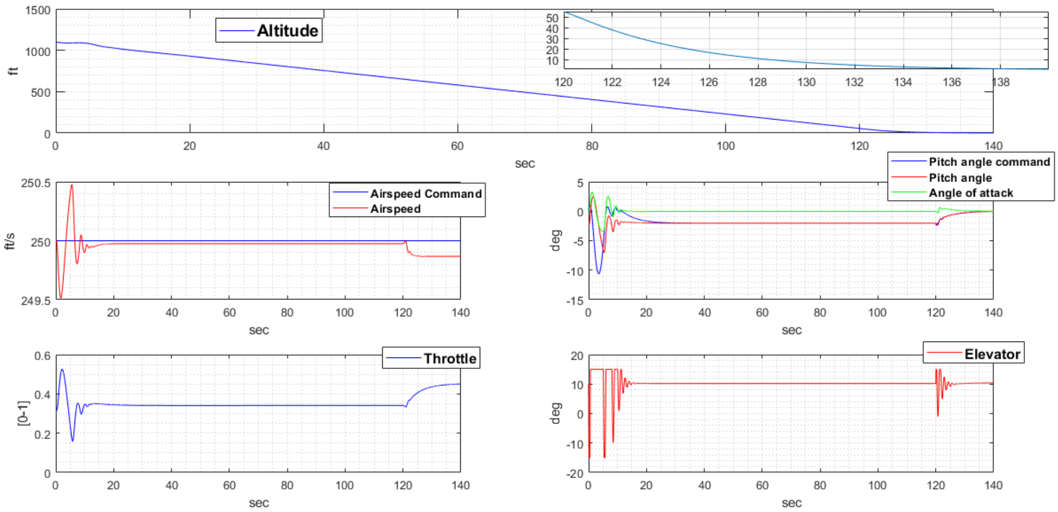

Figure 13: Simulation results for 0.1 seconds delay on pitch angle measurements.

be robust against sensor delays by achieving minimum phase margin of 45 degrees for critical loops. Nonlinear dynamics of transport aircraft is used to test designed controller. Simulation results show that desired trajectory is tracked accurately and aircraft performs a soft landing even in the case of large sensor delays.

References

Akmeliawati R. and Mareels I.M.Y. (2010) *Nonlinear Energy-Based Control Method for Aircraft Automatic Landing Systems*, IEEE Transactions on Cotrol Systems Technology, vol. 18, no. 4, July 2010

Blakelock J.H. (1991) *Automatic Control of Aircraft and Missiles*, John Wiley & Sons, 1991

Brown R., Romrell G., Johnson G., Kaufmann D., Qin X. (1996) *DGPS Category IIIb Auto-*

matic Landing System Flight Test Results, Proceedings of Position, Location and Navigation Symposium, Atlanta, USA, 1996

Buschek H. and Calise A.J. (1997) *Uncertainty modeling and fixed-order controller design for a hypersonic vehicle model*, Journal of Guidance Control and Dynamics, 20, pp.42–48, 1997

Cook M.V. (2013) *Flight Dynamics Principles: A Linear Systems Approach to Aircraft Stability and Control*, Elsevier, 2013

Juang J.G. and Chio J.Z. (2005) *Fuzzy modelling control for aircraft automatic landing system*, Proceedings of International Journal of Systems Science, Vol. 36, No. 2 pp. 77–87, February 2005

Liao F., Wang J.L., Poh E.K. and Li D. (2005) *Fault-Tolerant Robust Automatic Landing Control Design*, Journal of Guidance Control and Dynamics, vol. 28, no. 5, 2005

Stevens B.L., Lewis F.L. and Johnson E.N. (2016) *Aircraft Control and Simulation Dynamics, Control Design and Autonomous Systems*, John Wiley & Sons, 2016

www.mathworks.com, @1994-2017 The MathWorks, Inc.